



## CHAPTER II

### THEORETICAL BACKGROUND AND LITERATURE REVIEW

#### 2.1 Adsorption

Adsorption is the process through which a substance (adsorbate), originally present in one phase, is removed from that phase by accumulation at the interface between that phase and a separate phase (adsorbent). In principle, adsorption can occur at any solid-fluid interface such as gas-solid interface and liquid-solid interface (Armenante, 2011).

At the molecular level, adsorption is due to attractive interactions between a surface and the species being adsorbed or adsorbate. The magnitude of these interactions covers approximately two orders of magnitude (8–800 kJ/mole), similar to the range of interactions found between atoms and molecules in bulk phases. Generally, adsorption is classified according to the magnitude of the adsorption forces. Weak interactions (<40 kJ/mol) such as van der Waals forces are similar to those between molecules in liquids, called physical adsorption or physisorption. Strong interactions (>40 kJ/mol) such as covalent bonding are similar to those found between atoms within a molecule, called chemical adsorption or chemisorption. In physisorption, the adsorbed molecule remains intact but in chemisorption the molecule can be broken into fragments on the surface and this case is called dissociative chemisorptions ([en.wikipedia.org/wiki/Adsorption](http://en.wikipedia.org/wiki/Adsorption)).

In addition, the efficiency of adsorption depends on physical parameters such as temperature, pressure, and concentration in the bulk phase, and the surface area of the adsorbent, as well as on chemical parameters such as the elemental nature of the adsorbate and the adsorbent. For the good adsorption performance, low temperatures, high pressures, high surface areas, and highly reactive adsorbates or adsorbents are required ([www.answers.com/topic/adsorption](http://www.answers.com/topic/adsorption)).

In the separation process, the adsorptive separation is achieved by one of the three mechanisms including steric, kinetic, or equilibrium effect. The steric effect derives from the molecular sieving property of zeolites. In this case, only small and properly shaped molecules can diffuse into the adsorbent, while the other molecules

are totally excluded. The kinetic separation is achieved by virtue of the differences in diffusion rates of different molecules. The equilibrium separation processes is the large majority of processes operate through the equilibrium adsorption of the mixture. Some of the processes that use steric separation are listed in Table 2.1.

## 2.2 Selectivity

The primary requirement for an economic separation process is an adsorbent with sufficiently high selectivity, capacity, and life. The selectivity may depend on a difference in either adsorption kinetics or adsorption equilibrium and most of the adsorption processes in current use depend on equilibrium selectivity. In considering such processes, it is convenient to define a separation factor as follows equation:

$$\alpha_{AB} = \frac{X_A/X_B}{Y_A/Y_B}, \quad (2.1)$$

where  $X_A$  and  $Y_A$  are the mole fractions of component A in adsorbed and fluid phase at equilibrium, respectively. The separation factor defined in this way is precisely similar to the relative volatility, which measures the ease of separation by distillation. However, the analogy is purely formal and there is no quantitative relationship between the separation factor and relative volatility. For two given components, the relative volatility is fixed, while the separation factor varies widely depending on adsorbent (Ruthven, 1984).

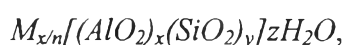
The separation factor generally varies with temperature and often also with composition, the choice of suitable conditions to maximize the separation factor is a major consideration in process design. It is certain that the higher the selectivity factor, the better the effect of the separation between two components (Guo *et al.*, 2000). For an ideal Langmuir system, the separation factor is independent of composition and equal to the ratio of the Henry's law constants of the two relevant components.

**Table 2.1** Steric separations by molecular-sieve zeolites (Yang, 1987)

Molecular-Sieve Basic Type	Molecules Adsorbed	Molecules Excluded	Typical Applications
3A	H <sub>2</sub> O, NH <sub>3</sub> , He (molecules with an effective diameter <3 Å)	CH <sub>4</sub> , CO <sub>2</sub> , C <sub>2</sub> H <sub>2</sub> , O <sub>2</sub> , C <sub>2</sub> H <sub>5</sub> OH, H <sub>2</sub> S (molecules with an effective diameter >3 Å)	Drying cracked gas, ethylene, butadiene, and ethanol
4A	H <sub>2</sub> S, CO <sub>2</sub> , C <sub>2</sub> H <sub>6</sub> , C <sub>3</sub> H <sub>6</sub> , C <sub>2</sub> H <sub>5</sub> OH, C <sub>4</sub> H <sub>6</sub> (molecules with an effective diameter <4 Å)	C <sub>3</sub> H <sub>8</sub> , compressor oil (molecules with an effective diameter >4 Å)	Drying natural gas, liquid paraffins and solvents. CO <sub>2</sub> removal from natural gas
5A	<i>n</i> -Paraffins, <i>n</i> -olefins, <i>n</i> -C <sub>4</sub> H <sub>9</sub> OH (molecules with an effective diameter <5 Å)	Iso-compounds, all 4 + carbon rings (molecules with an effective diameter >5 Å)	<i>n</i> -Paraffin recovery from naphtha and kerosene
10X	Iso-paraffins, iso-olefins (molecules with an effective diameter <8 Å)	Di- <i>n</i> -butylamine and larger (molecules with an effective diameter >8 Å)	Aromatic separation
13X	Di- <i>n</i> -butylamine (molecules with an effective diameter <10 Å)	(C <sub>4</sub> F <sub>9</sub> ) <sub>3</sub> -N (molecules with an effective diameter >10 Å)	Desulfurization, general drying, simultaneous H <sub>2</sub> O and CO <sub>2</sub> removal

### 2.3 Zeolites

Zeolites are porous crystalline aluminosilicates. The framework consists of tetrahedral aluminium and silicon atoms bridged by oxygen atoms. The zeolite can be represented by the stoichiometry:



where  $x$  and  $y$  are integers with  $y/x$  equal to or greater than 1,  $n$  is the valence of cation  $M$ , and  $z$  is the number of water molecules in each unit cell. Unit cells are shown in Figure 2.1(a) and 2.1(b). The presence of aluminium atoms introduces charge defects, which are compensated with some non-framework cations such as sodium, potassium, calcium, and barium. The water molecules can be removed with ease upon heat and evacuation, leaving an almost unaltered aluminosilicate skeleton with a void fraction between 0.2 and 0.5. The skeleton has a regular structure of cages, which are usually interconnected by six windows in each cage. The cage can imbibe or occlude large amounts of guest molecules in place of water. The size of the window apertures ranges from 3 Å to 10 Å and it can be controlled by fixing the type and number of cations. The size of the aperture and the surface property in the cages can affect the selectivity.

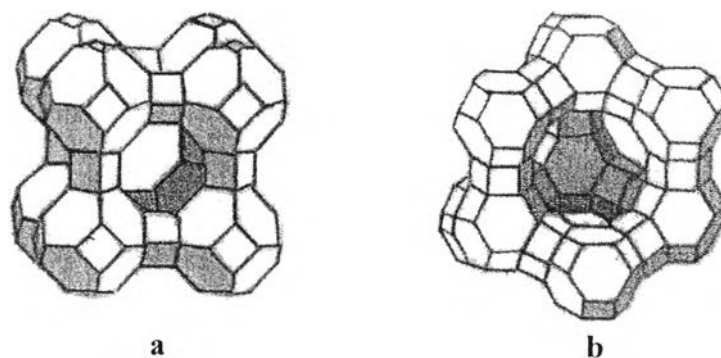


**Figure 2.1** Zeolite structure; (a) unit cell of type A zeolite; (b) unit cell of type X and Y, or faujasite zeolite.

(<http://minmag.geoscienceworld.org/content/vol64/issue1/images/small/gsmminmag.64.1.1fig2.gif>)

The primary structural units of zeolites are tetrahedral of silicon and aluminum,  $\text{SiO}_4$  and  $\text{AlO}_4$ . These units are assembled into secondary polyhedral building units such as cubes, hexagonal prisms, octahedral, and truncated octahedral. The silicon and aluminum atoms, located at the corners of the polyhedral, are joined by a shared oxygen. The final zeolite structure consists of assemblages of the secondary units in a regular three-dimensional crystalline framework. The ratio  $\text{Si}/\text{Al}$  is commonly one to five. The aluminum atom can be removed and replaced by silicon in some zeolites and this causes the number of cations to decrease. Moreover, the non-framework cations can also be exchanged. The inner atoms in the windows are oxygen and the size of the windows depends on the number of oxygen atoms in the ring – four, five, six, eight, ten, or twelve. The aperture size, as well as the adsorptive properties, can be further modified by the number and type of exchanged cations. There are many types of zeolite such as type A, type X, type Y and type ZSM (Yang, 1987).

Among the hundreds of zeolites known to date, the X and Y faujasite zeolites are of great interest because of their relevance to industrial processes. The alkali metal ion-exchanged faujasite zeolites can be used to catalyze the side chain alkylation of aromatic compounds such as toluene and ethylbenzene, while the acidic forms can selectively catalyze ring alkylation. Besides alkylation, faujasite zeolites can also be utilized to separate xylene isomers and the preference to a specific xylene isomer depends on the nature of the cations in the framework (Zhu *et al.*, 2008). The Parex unit is one of the industrial processes that use faujasite zeolite, including KY and BaX to separate xylene isomers. In this research, only the X and Y faujasite zeolites will be focused on. They are the most interesting zeolites for  $\text{C}_8$  aromatics separation.

The skeleton structure of types X and Y zeolites are the same as that of the naturally occurring faujasite, which display cubic crystalline lattices. The microporous network is made of cuboctahedral sodalite cages with a diameter of about 6.5 Å. These cages are linked together in a tetrahedral arrangement by six oxygen atom rings (six-member prisms) and form large cavities, which have a diameter of about 12.5 Å, named supercages, as shown in the unit cell in Figure 2.1(b). Each unit cell contains 192 (Si, Al) $\text{O}_4$  tetrahedra. The number of aluminum

ions per unit cell varies from 96 to 77 for type X zeolite, and from 76 to 48 for type Y zeolite. This framework has the largest central cavity volume of any known zeolite, amounting to about 50% void fraction in the dehydrated form. A unit cell, when fully hydrated, contains approximately 235 water molecules, mostly in the central cavity. The aperture is formed by the twelve-member oxygen rings with a free diameter of approximately 7.4 Å. One cubic unit cell contains 8 sodalite cages and 8 supercages. Three major locations for the cations are indicated in Figure 2.2. The locations are: center of the six-member prism (I) and opposite to I in the sodalite cage (I'); similar to I and I' but further from the central cavity (II and II'); and at the twelve-member aperture (III and III'). The ratio of silicon to aluminium atoms and the number of cations vary from one faujasite to another. A faujasite is named Y when it has a Si/Al ratio greater than 1.5. In the other hand, it is named X when it has a Si/Al ratio lower than 1.5 (Lachet *et al.*, 2001).

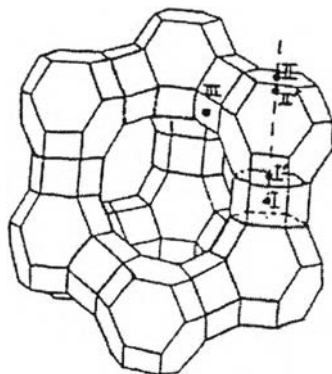


**Figure 2.2** Cation sites in types X and Y (16 I, 32 I', 32 II, 32 II', 48 III, and 32 III' sites per unit cell). (<http://www.freepatentsonline.com/6780806.html>)

## 2.4 Headspace Chromatography

Headspace gas chromatography (HS-GC) is used for the analysis of volatiles and semi-volatile organics in solid, liquid, and gas samples. This technique has been used since the 1930s (Harger *et al.*, 1939), but only recent year, it has become popular and now gained worldwide acceptance for analyses of alcohols in

blood and residual solvents in pharmaceutical products. Moreover it can be used to analysis flavour compounds in beverages and food products, fragrances in perfumes and cosmetics, and the monomers in polymers and plastic ([www.labhut.com](http://www.labhut.com)). In addition, this technique was used to study  $C_8$  aromatics adsorption (Torres *et al.*, 2001).

Generally, headspace technique is suitable for the analysis of the very light volatiles in samples that can be efficiently partitioned into the headspace gas volume from the liquid or solid matrix sample. In the part of higher boiling volatiles and semi-volatiles, which have low partition in the gas headspace volume, they are not detectable with this technique. Furthermore, this technique is also proper for complex sample matrices, which require sample preparation or extraction or difficult to analyze directly, because they can be placed directly in a vial with little preparation

This technique has many advantages such as clean, easy sample preparation, saves both time and money, and is good for quality control or sample screening. This is made possible by modern instrumentation being able to reproducibly prepare samples in an efficient manner ([www.labhut.com](http://www.labhut.com)).

#### 2.4.1 Basic Principles of Headspace Analysis

Headspace analysis is the qualitative and quantitative analysis of a gas in equilibrium with a liquid or solid sample in a closed vessel (Wang *et al.*, 2008). The methodology for headspace is quite simple. A headspace sample is normally prepared in a vial containing the sample, the dilution solvent, a matrix modifier, and the headspace. The complex sample mixture is thermostated for a period of time to allow the solvents in the matrix to volatilize and isolated in the headspace or gas portion of a sample vial. The gas phase in a chromatography vial above the sample is called headspace, which is sampled and injected into a GC system for separation of all of the volatile components. The phases of the headspace vial are shown in Figure 2.3.

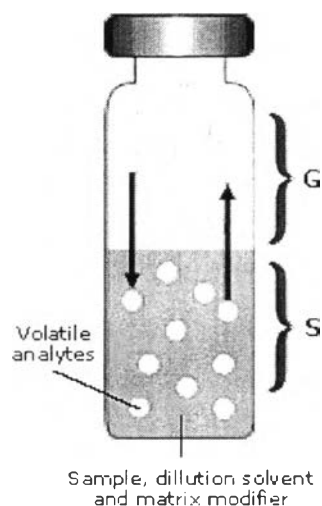


**Figure 2.3** Phases of the Headspace Vial. (www.labhut.com)

Where G is the gas phase, which is commonly referred to as the headspace and lies above the condensed sample phase, and S is the sample phase, which contains the compound(s) of interest and is usually in the form of a liquid or solid in combination with a dilution solvent or a matrix modifier.

Once the sample phase is introduced into the vial, and the vial is sealed, volatile components diffuse into the gas phase until the headspace has reached a state of equilibrium as depicted by the arrows. The sample is then taken from the headspace. Therefore, vial size and septa are important for the experiment.

Headspace sample vials are available in 6, 10 and 20 mL sizes. A vial should be large enough to ensure adequate headspace or phase ratio without excessive dilution of the components of interest. About the sample volume, for headspace technique, more sample volume does not always provide the expected increase in area counts because the greater the sample volume, the smaller the actual headspace volume becomes, as shown in Figure 2.4 (Kott and Chen, 2010). Septa should be suitable for the temperature of the system because the poor septa can cause bleed and so contaminate the headspace.



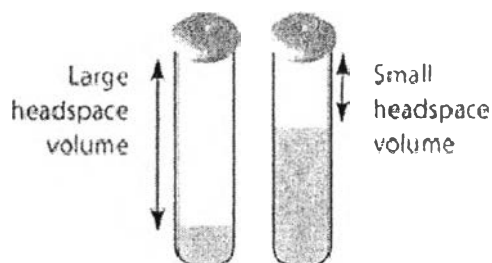


**Figure 2.4** Effects of sample volume on the volume of headspace in sample vials.  
(Kott and Chen, 2010)

One of the important factors in the headspace GC method is incubation time because it affects solvent-vapor equilibria, which play a role in the headspace analysis. The more readily a solvent can be evaporated into the headspace means the more of that particular solvent will be injected into the column. If the sample is incubated for too short a period of time, the headspace will have less of the analyte, and this can affect overall area counts. After a certain point, however, the analyte and the solution, from which it came, will settle into equilibrium. On the other hand, the more incubation will not result in any more samples entering the vapor phase and may result in sample degradation or cause secondary reactions.

#### 2.4.2 Partition Coefficient

The partition coefficient is the equilibrium distribution of an analyte between the sample phase and the gas phase. Normally, samples must be prepared to maximize the concentration of the volatile components in the headspace and minimize unwanted contamination from other compounds in the sample matrix. Moreover, the partition coefficient can be used to determine the concentration of an analyte in the headspace and can be calculated as the following equation.

$$\text{Partition Coefficient } (K) = C_s/C_g, \quad (2.2)$$

where  $C_s$  is the concentration of analyte in the sample phase and  $C_g$  is the concentration of analyte in the gas phase. The low  $K$  values mean that the compound

will tend to partition more readily into the gas phase and have relatively high responses and low limits of detection. On the contrary, the compounds that have high K values will tend to partition less readily into the gas phase and have relatively low responses and high limits of detection. Partition coefficient (K) values for other common compounds are shown in the Table 2.2. Besides, the partition coefficient can affect to the sensitivity. When the partition coefficient is decreased, volatiles can more readily enter the gas phase and sensitivity is increased as illustrated by Figure 2.5. The partition coefficient can be lowered by changing the temperature, at which the vial is equilibrated or by changing the composition of the sample matrix or by changing the phase ratio.

**Table 2.2** Partition coefficient (K) values of common solvents in air-water systems at 40 °C (www.labhut.com)

<b>Solvent</b>	<b>K Value</b>
<b>cyclohexane</b>	0.077
<b>n-hexane</b>	0.14
<b>tetrachloroethylene</b>	1.48
<b>1,1,1-trichloromethane</b>	1.65
<b>o-xylene</b>	2.44
<b>toluene</b>	2.82
<b>benzene</b>	2.90
<b>dichloromethane</b>	5.65
<b>n-butyl acetate</b>	31.4
<b>ethyl acetate</b>	62.4
<b>methyl ethyl ketone</b>	139.5
<b>n-butanol</b>	647
<b>isopropanol</b>	825
<b>ethanol</b>	1355
<b>dioxane</b>	1618

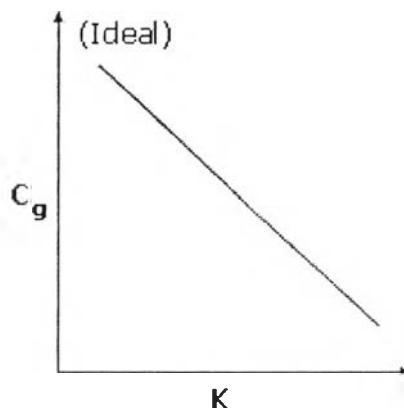


**Figure 2.5** The relation between K value and sensitivity (www.labhut.com).

#### 2.4.3 Phase Ratio

The phase ratio is defined as the relative volume of the headspace compared to volume of the sample in the sample vial. The calculation of phase ratio value is shown in Equation (2.3).

$$\text{Phase Ratio } (\beta) = V_g / V_s, \quad (2.3)$$

where  $V_s$  is the volume of sample phase, and  $V_g$  is the volume of gas phase. The relation between sensitivity and phase ratio is the same as shown in the partition coefficient part. Usually, lower values of  $\beta$  will yield higher responses for volatile compounds and higher sensitivity. But sometime, decreasing the  $\beta$  value will not always yield the increase in sensitivity. Because when  $\beta$  is decreased by increasing the sample size, compounds with high K values partition less into the headspace compared to compounds with low K values and yield correspondingly smaller changes in  $C_g$ . So the samples that contain compounds with high K values need to be optimized to provide the lowest K value before changes are made in the phase ratio.

#### 2.4.4 Combining Partition Coefficient and Phase Ratio

Partition coefficients and phase ratios are combined to determine the final concentration of volatile compounds in the headspace of sample vials. The concentration of volatile compounds in the gas phase can be expressed as

$$C_g = C_o / (K + \beta), \quad (2.4)$$

where  $C_g$  is the concentration of volatile analytes in the gas phase, and  $C_o$  is the original concentration of volatile analytes in the sample. To get the higher concentrations of volatile analytes in the gas phase and better sensitivity, the lowest values for both  $K$  and  $\beta$  are needed.

#### 2.4.5 Classification of Headspace Sampling Techniques

The key in headspace GC is the sampling and transfer of the samples in headspace to GC (Zhu and Chai, 2005). There are various techniques of headspace sampling such as static HS-GC, dynamic HS-GC, and Solid Phase Microextraction (SPME), which approach for the removal and sampling of volatile chemicals from condensed matrices. These methodologies use different instrumentation and employ different quantification techniques (Markelov and Bershevits, 2001). In this research, static headspace is described in more details.

##### *2.4.5.1 Static Headspace Gas Chromatography*

Static headspace GC was the earliest developed and is the most mature headspace technique. This instrument is a primary tool for the analysis of volatile organic compounds in environmental samples, flavors, and fragrances (Wang *et al.*, 2008). Traditional static HS-GC relies on the vapor-liquid equilibrium (VLE) of a volatile compound in a nonvolatile matrix within a closed container (vial) for determining the concentration of the volatile compound in the sample (Zhu and Chai, 2005). This method does not require complete removal of analyte from its matrix for quantification. Only a portion of the analyte that corresponds to its equilibrium concentration has to reach the vapor phase and be sampled (Markelov and Bershevits, 2001). However, there is some limited sensitivity; thus, the static HS-GC is mostly useful for applications in the high-ppb to percent concentration ranges.

A peculiar problem in static HS-GC is the internal pressure in the headspace vial generated during thermostating by the sum of partial vapor pressures from all volatile sample constituents, from which in general the humidity

of the sample is predominant. Thus, the vapor pressure of water contributes mostly to the internal pressure. Moreover, some sampling techniques pressurize the vial prior to sample transfer with the inert carrier gas. For these reasons, it is necessary to close the vial pressure tight by a septum (preferably PTFE-lined) and to crimp-cap it by an aluminum cap (Kolb, 1999).

There are three types of static headspace autosamplers including syringe injection, pressurized loop, and balance pressure. The most popular and common method of headspace sampling is a syringe injection. This method has three steps. Step 1, the syringe is heated in an oven for a pre-defined period of time. Moreover, it must be heated above the temperature of the oven to avoid the risk of condensation and hence carry-over from one sample to the next. Then, the heated syringe removes an aliquot of the headspace (step 2) and injects it directly into the GC (step 3). After injection, the syringe is flushed with nitrogen or other inert gas. This method is illustrated in Figure 2.6.

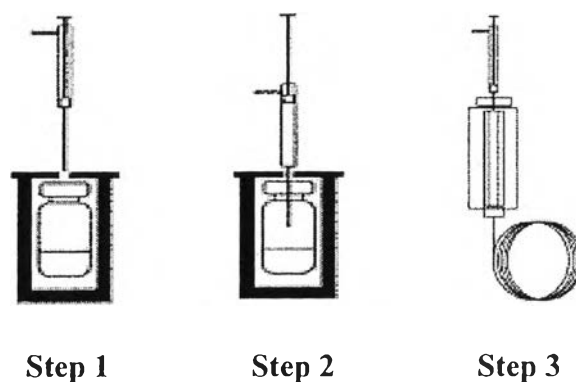


**Figure 2.6** Schematic of the syringe injection headspace sampling system. Step 1: sample reaches equilibrium, step 2: sample is extracted from the headspace, and step 3: sample is injected. (www.labhut.com)

The syringe injection system has many advantages such as very high level of reproducibility, low carry-over, fast transfer of sample to GC, precise control of sample syringe for sample size and injection speed, and easy to clean syringe. However, there is the inherent problem that the internal pressure in the vial extends into the barrel of the syringe and after withdrawal from the vial, the

pressurized headspace gas then expands through the open needle to the atmosphere. Part of the headspace gas will thus be lost. This problem may be avoided by using a gas-tight syringe equipped with a valve. Such syringes may be adequate for manual sampling, but are hard to automate.

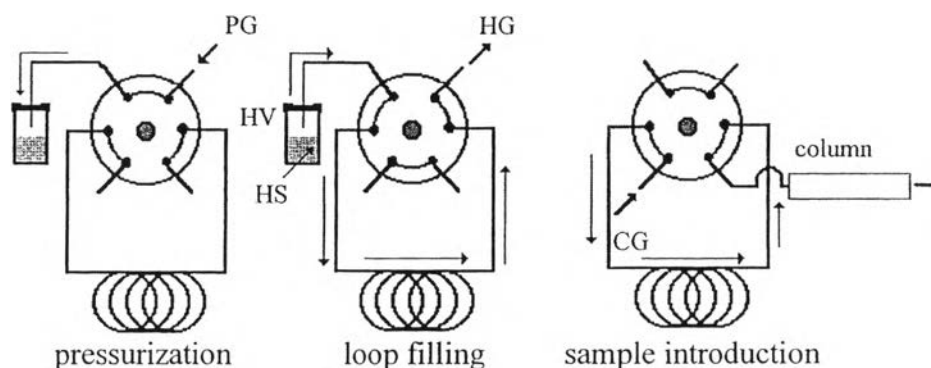


**Figure 2.7** Schematic of the pressurized loop headspace sampling system. PG - Pressurization gas, HV = headspace vial, HS = headspace sample, and CG = carrier gas. (Kolb, 1999)

The second headspace sampling system, pressurized loop system comprises of gas sampling valves (typically uses a six-port valve) with sample loops and uses a known amount of sample. Filling the loop with headspace gas is achieved by pressurizing the vials first up to a certain pressure level above the original pressure in the vial. After pressurization, the valve is turned and the loop is filled with the headspace gas. Once the loop has been filled, the valve is turned again to redirect the gas flow and flush the sample into the transfer line leading to the analytical column as shown in Figure 2.7. This system can be used at high temperatures but it also has some problems such as sample carry over, and the injection port is always occupied.

Figure 2.8 shows the schematic of balanced pressure system. This system uses a seamless injection directly from the vial into the carrier gas stream and needs only valve and needle. Initially, it uses an incubation oven to thermostat the vial, thus, the sample reaches equilibrium. During this step, the inert carrier gas enters the gas chromatograph through a solenoid valve and branches

before the column. Some of the carrier gas is directed to the sampling needle. The needle is inserted into the vial and is then pressurized with a carrier gas. After that, the sample is transferred through the closing solenoid valve for few seconds and the carrier gas flow is disconnected. Then, the pressurized headspace gas in the vial expands now directly into the column without loss of headspace gas to atmosphere. The headspace gas replaces the carrier gas flow during the sampling time and the volume of headspace gas transferred into the column is therefore time-controlled, and the injected volume can precisely be adjusted by varying the sampling time in a wide range. This technique can be quite accurate but has some disadvantages as in pressurized loop system.

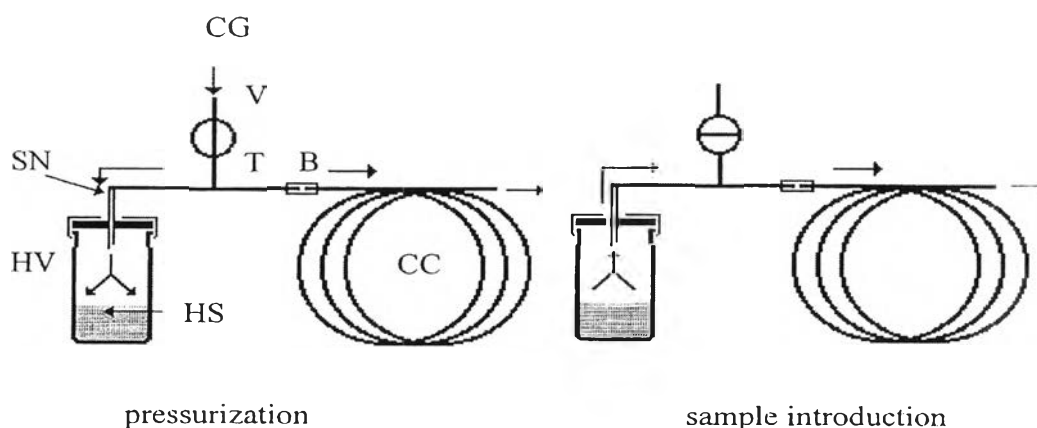


**Figure 2.8** Schematic of the balanced pressure headspace sampling system in splitless configuration. CG = Carrier gas, V = solenoid valve, SN = sampling needle, HV = headspace vial, HS = headspace sample, T = fused-silica transfer line, B = butt connector, and CC = capillary column. (Kolb, 1999)

#### 2.4.5.2 Dynamic Headspace Gas Chromatography

The dynamic headspace GC is known as *purge-* and *-trap* method. This technique separates the volatile sample constituents from the sample by a continuous flow of an inert gas either through or above a solid or liquid sample and delivers them onto the trap. Then, trapped chemicals are thermally desorbed from the trap into a gas chromatograph. The quantification requires the complete removal of the chemicals from the sample. In many cases, this is difficult to achieve in

reasonable time, especially for solids, where the bubbling of gas through the sample is not possible (Markelov and Bershevits, 2001). Moreover, this technique is very sensitive (low ppb to ppm level) and has limit of sample which prefer to liquid (Wang *et al.*, 2008).

## 2.5 Literature Review

Santacesarla *et al.* (1982) studied the separation of C<sub>8</sub> aromatics on potassium exchanged Y zeolite through Finite Bath Experiments. The adsorption equilibrium parameters, selectivities, and mass transfer coefficients were investigated. The adsorption for a single-component can be well interpreted by using the Langmuir and Fowler isotherms. For multi-component adsorption, both isotherms can be used to interpret the experimental data when total coverage,  $\theta_{\text{tot}} > 0.5$  but when  $\theta_{\text{tot}} < 0.5$ , the Fowler isotherm is more suitable. The trend of equilibrium constant value of each component on KY was consistent with the *p*-xylene selectivity, and the most adsorbed species had the highest K value. For kinetics of adsorption, the adsorption rate of the zeolite powder was very high and the kinetic parameters are difficult to evaluate accurately. In the part of zeolite pellet, the diffusion rate in the microcrystals was very high due to the small size of the crystal. The rate determining step is the internal diffusion from the surface to the macropores of the pellet.

Medium-pore ZSM-5 zeolites were used as adsorbent for separation of *p*-xylene and ethylbenzene from C<sub>8</sub> aromatics by Yan (1989). The experiments were done at 25 °C, and mesitylene was used as diluents and internal standard in GC analysis. Moreover, the effect of SiO<sub>2</sub>/Al<sub>2</sub>O<sub>3</sub> ratio was investigated. The result showed that the medium-pore ZSM-5 zeolite is highly selective for *p*-xylene adsorption. The selectivity for *p*-xylene over ethylbenzene varied with *p*-xylene and total hydrocarbon loading on the zeolite, while the selectivity for *p*-xylene over *o*-xylene showed to be rather constant. The selectivity for *p*-xylene over ethylbenzene was 5.5 at SiO<sub>2</sub>/Al<sub>2</sub>O<sub>3</sub> ratio of 700, which is the optimum ratio. The high *p*-xylene selectivity and its dependence on *p*-xylene loading were related to the unique packing of *p*-xylene in the crystalline cavities. The total adsorption capacity was



between 160 and 190 mg/g and the competitive adsorption capacity for *p*-xylene from a simulated reformer product was 120 mg/g.

In 1990, Barthomeuf and Mallmann studied the adsorption of benzene and *o*-xylene by means of infrared spectroscopy on  $\text{AlPO}_4\text{-5}$  and NaY. For  $\text{AlPO}_4\text{-5}$ , these aromatics did not interact strongly with the  $\text{AlPO}_4\text{-5}$  structure, but changes in the packing of these molecules altered the shape of the infrared spectra.  $\text{AlPO}_4\text{-5}$  was selective for *o*-xylene and the selectivity in the separation of  $\text{C}_8$  aromatics was related to the packing of molecules and consequently their cohesive energy. On NaY, a strong cation- $\pi$  electron interaction was observed for the two hydrocarbons and for other aromatics. The selectivity of benzene and  $\text{C}_8$  aromatics by strong adsorption on NaY was related to the aromatic-zeolite interaction, which disturbed the adsorbed molecules. NaY was selective for *m*-xylene over the other  $\text{C}_8$  aromatics because *m*-xylene is the most basic, which strongly interact with the acidic  $\text{Na}^+$  ions.

The thermodynamic and kinetics of adsorption were studied by Hulme *et al.* (1991). They found that there is no fundamental thermodynamic difference between liquid and vapor adsorption because the composition of an adsorbed phase in equilibrium with a liquid must be precisely the same. On the contrary, the main difference between the adsorption in gas phase and liquid phase is shown in kinetics. Mass transfers to the adsorption sites in the liquid phase are much slower than that in gas phase, but the selectivity and the adsorption capacity are the same order of magnitude. Moreover, there is the difference in loading. The total adsorbed phase concentration is always at or near the saturation limit in the liquid phase, while the vapor phase adsorption studies are generally carried out at relatively low loading.

The adsorption processes of *p*-xylene and *m*-xylene on Y zeolite was studied by Bellat *et al.* (1997). At 25 °C, the adsorption capacity of  $\alpha$ -cages was nearly the same for both xylene and was not changed by cation exchange with potassium or barium. The amount of *p*-xylene adsorbed on Y zeolite was up to 13% of the total amount adsorbed at saturation, and that was twice greater than *m*-xylene. However, they reported that the adsorption capacity depended on the compensation cation, temperature, and pressure.

The binder-free MFI zeolite, which possesses perfect framework and high hydrophobicity, was used as an adsorbent to study the static equilibrium of  $\text{C}_8$

aromatics in liquid phase by Guo *et al.* (2000). A series of desorbents matched with adsorbent were investigated. They found that the *n*-butylbenzene was the best desorbent because it can be used to desorb efficiently by the less volume. Moreover, mesitylene (TMB) was used as an inert component due to its molecular size, which cannot enter the pores of the zeolite. The binder-free MFI zeolite has smaller pores than ZSM-5 zeolite and high shape selectivity of separation, thus, the saturation adsorptive capacities of *m*-xylene and *o*-xylene are much less than those of *p*-xylene and ethylbenzene. The selectivity factor of *p*-xylene/ethylbenzene and *p*-xylene/*o*-xylene was 7.95 and 104, respectively. In part of *m*-xylene, it was not adsorbed by zeolite, so the selectivity factor of *p*-xylene/*m*-xylene was not reported. This adsorbent can be used without controlling the water content and regenerated up to 100 times. In addition, its adsorptive capacity of *p*-x is greater than faujasite type zeolite, BaX, at the same concentration of equilibrium of *p*-xylene.

Two experimental complementary techniques, GC and GC-C-IRMS, were used together to study the adsorption of a binary liquid mixture *p*-xylene and *m*-xylene on a dehydrated KBaY zeolite by Tournier *et al.* (2000). GC was used to measure selectivities in the concentration range of 3-95% *p*-xylene, while GC-C-IRMS was used to measure in range of 0-3% and 95-100% *p*-xylene. The experiments were done at 150 °C, and used isooctane as an inert. From the experiments, KBaY was selective for *p*-xylene in the whole compositional range. The *p*-xylene selectivity depended on the composition of the liquid phase. The selectivity increased strongly when the mixture became lean in *p*-xylene, but it was close to unity when the mixture became rich in *p*-xylene. Moreover, the Langmuir-Freundlich model was applied to competitive adsorption in the liquid phase. This model was possible to predict the adsorption equilibrium of a xylene mixture in the concentration range of 0.1%-99.7% *p*-xylene.

The single- and multi-component liquid phase adsorption of C<sub>8</sub> aromatics was studied using BaY zeolite and headspace chromatography technique at 60 °C by Torres *et al.* (2000). From the single component liquid adsorption data, BaY zeolite more strongly adsorbed *p*-xylene than *n*-decane. The results of headspace and finite bath technique were in reasonable agreement for full concentration range. But at low concentration range, the result from the finite bath method seemed inherit error. The

headspace measurements show a decreasing relative equilibrium vapor pressure for the more strongly adsorbed species (*p*-xylene) and an increasing relative pressure for the less strongly adsorbed species (*o*-xylene) as saturation loading is approached and the micropore capacity is about 13 wt%. The selectivity of *p*-xylene with respect to *o*-xylene is about 5.7 at 60 °C. It was concluded that the headspace method provides a simple and useful technique for measuring both single-component isotherms and separation factors for multi-component liquid mixture.

In 2000, Ngamkitidachakul investigated the effects of initial concentration and temperature on the C<sub>8</sub> aromatics adsorption by using KY and KBaX zeolites as adsorbent and toluene as desorbent. The result showed that KY adsorbed more *p*-xylene and toluene than KBaX did. For KY zeolite, *p*-xylene was adsorbed more than other species, while *o*-xylene was the least adsorbate at high xylene/toluene ratios. For KBaX zeolite, the experimental result was the same trend as KY zeolite at high xylene/toluene ratios whereas *o*-xylene was the most adsorbed one at low xylene/toluene ratios. Adsorption of C<sub>8</sub> aromatics decreased when the temperature increased. Moreover, the transfer rate was low as the temperature decreased. However, temperature has very little effect on selectivity of *p*-xylene with respect to other C<sub>8</sub> aromatics for both zeolites at full capacity.

Liquid phase adsorption of C<sub>8</sub> aromatics in the presence of toluene on KY and KBaX zeolites was studied by Varayanond (2001). It was found that KY zeolite can adsorb more capacity than KBaX zeolite and both of them adsorbed more *p*-xylene, followed by ethylbenzene, *m*-xylene and *o*-xylene. The adsorption efficiency and selectivity was high at low operating temperature because the adsorption is exothermic. On the other hand, the molecular transfer rate was low at low temperature. When the water content in zeolite increased, the adsorption capacity and *p*-xylene selectivity decreased. Moreover, he reported that both zeolites can adsorb *p*-xylene more than toluene but adsorb toluene more than *m*-xylene and *o*-xylene. In addition, multi-component pulse test on KY zeolite at low concentration was tested. The result showed that the selectivity of *p*-xylene over *m*-xylene was the highest, and the selectivity from the pulse test was higher than selectivity from the single component experiment.

The acid-base interaction between the C<sub>8</sub> aromatics and the zeolites was studied using X and Y zeolite by Suntornpun (2002). For both X and Y zeolite, the acidity increased as Cs, Rb, K, Na and Li exchanged zeolites, while the ionic radius decreased as Cs, Rb, K, Na and Li. However, the acid-base interaction theory was not sufficient to explain the adsorption behavior of C<sub>8</sub> aromatics for all cations. The selectivity was affected from both the acid-base interaction and the exchanged cation size. For both of dynamic adsorption and equilibrium adsorption, KY had high selectivity of *p*-xylene. Moreover, the heat of adsorption was also studied, and the result showed that *p*-xylene had highest  $\Delta H$  followed by ethylbenzene, *o*-xylene, and *m*-xylene.

Effects of zeolite acidity on C<sub>8</sub> aromatics adsorption was studied by Limsamutchaikul (2003). The difference zeolites, 2.0X, 2.5X, Y, and difference exchanged cations, Ba, Sr, Ca, Mg, were used to investigate acidity effect with pulse test and breakthrough technique.  $S_{int}$ , the intermediate electronegativity, was used to represent zeolite acidity. The higher  $S_{int}$  means the higher acidity. At the same Si/Al<sub>2</sub> ratio, when the cation size decreased from Ba, Sr, Ca and Mg, the zeolite acidity increased. By varying the Si/Al<sub>2</sub> ratio, zeolite acidity increased from 2.0X, 2.5X and Y zeolite. For the pulse test technique result, the *p*-xylene selectivity with respect to *m*-xylene and *o*-xylene of X zeolite were controlled by both acid-base interaction and exchanged cation size. In the part of *p*-xylene selectivity with respect to ethylbenzene, the selectivity was controlled by acid-base interaction only. The trends of *p*-xylene selectivity with respect to the other C<sub>8</sub> aromatics on the Y zeolite are the same as that on the X zeolite. For the breakthrough technique result, the same trend as in the pulse test results were obtained but the acid-base interaction did not play an important role on the Y zeolite. As the result, the *p*-xylene selectivity decreased as the zeolite acidity increased and the Ba2.5X had the highest *p*-xylene selectivity.

In 2005, Buarque *et al.* studied adsorption equilibrium of C<sub>8</sub> aromatic liquid mixture on BaY zeolites using headspace chromatography technique and focusing on multi-component equilibrium models. The experiment was performed at 80-120 °C. The results showed that the selectivities between *p*-xylene and the other C<sub>8</sub> aromatics decreased almost linearly with increasing temperature and the liquid/solid ratio of about 13 wt% was achieved at saturation. Langmuir (L) and Dual-site Langmuir

(DSL) equilibrium models were used to evaluate the pure component experimental data. Both Langmuir and DSL models can be used to describe the pure component adsorption but the DSL model fit the data somewhat better than the Langmuir model. From pure component data, the multi-component equilibrium models, Ideal Adsorbed Solution (IAS) model and Extended Langmuir Multi-component model, were tested to correlate the data. The IAS model did not represent well the C<sub>8</sub> aromatics adsorption on the Y zeolite for multi-component behavior due to the nonideality of the adsorbed phase, while the Extended Langmuir model provided an adequate and numerically convenient way to predict multi-component equilibrium and better agreement with the experimental equilibrium data for C<sub>8</sub> aromatics on Y zeolite.

The headspace technique was used by Luna *et al.* (2010) to study C<sub>8</sub> aromatic adsorption in BaY and mordenite molecular sieves. BaY strongly adsorbed *p*-xylene and gave high *p*-xylene selectivity for both binary and quaternary mixture of C<sub>8</sub> aromatic isomers. The results from the headspace and chromatographic were in good agreement. On the other hand, mordenite adsorbed *o*-xylene and *o*-xylene selectivity was 1.7 at 40 °C. The adsorption capacity of mordenite was much smaller than the adsorption capacity of BaY zeolite, and decreased with temperature. Moreover, the influence of xylene concentration was investigated, and the result showed that the selectivity values were not significantly affected by the relative concentration of the xylene isomers.